Neutron diffraction study of stability and phase transitions in Cu-Sn-In alloys as alternative Pb-free solders

G. Aurelio, S. A. Sommadossi, and G. J. Cuello

Citation: J. Appl. Phys. **112**, 053520 (2012); doi: 10.1063/1.4751019
View online: http://dx.doi.org/10.1063/1.4751019
View Table of Contents: http://jap.aip.org/resource/1/JAPIAU/v112/i5
Published by the American Institute of Physics.

Neutron diffraction study of stability and phase transitions in Cu-Sn-In alloys as alternative Pb-free solders

G. Aurelio,[1,a)] S. A. Sommadossi,[2] and G. J. Cuello[3]
[1]*Consejo Nacional de Investigaciones Científicas y Técnicas, Centro Atómico Bariloche-Comisión Nacional de Energía Atómica, Av. Bustillo 9500, 8400 S. C. de Bariloche, RN, Argentina*
[2]*IDEPA–Consejo Nacional de Investigaciones Científicas y Técnicas–Facultad de Ingeniería, Universidad Nacional del Comahue, Buenos Aires 1400, 8300 Neuquén, Argentina*
[3]*Institut Laue Langevin, F-38042 Grenoble, France*

(Received 2 May 2012; accepted 9 August 2012; published online 12 September 2012)

In this work, we present an experimental study of structure and phase stability of ternary Cu-Sn-In alloys around 55 at. % Cu in the temperature range $100\,^{\circ}\mathrm{C} \leq T \leq 550\,^{\circ}\mathrm{C}$. We have followed the real-time sequence of phase transformations in succesive heating and cooling ramps, using state-of-the-art neutron powder thermodiffractometry, complemented with calorimetric studies of the phase transitions. Our results give experimental support to the current assessment of the ternary phase diagram in this composition and temperature range, confirming the sequence of transitions $\eta \rightarrow (\eta + L) \rightarrow (\varepsilon + L)$ with transformation temperatures of 210 °C and 445 °C, respectively. The use of neutrons allowed to overcome common difficulties in phase identification with powder XRD due to absorption and preferred orientation issues. Even the transitions to liquid phases could be successfully identified and monitored *in situ*, turning the neutron thermodiffraction technique into a valuable tool for phase diagram studies of emerging lead-free solder candidates. © *2012 American Institute of Physics*. [http://dx.doi.org/10.1063/1.4751019]

I. INTRODUCTION

Sn-based alloys have gained increasing attention in the last years, especially since the implementation of regulations to eliminate Pb from the electronic industry. Tin, the most used Pb replacement, forms intermetallic phases (IPs) with most conductor metals. These IPs usually form a layer between the metallic substrate and the solder alloy, which is indicative of a good metallurgical bond. Despite their essential presence in the bonds, IPs must be carefully monitored, because they are often brittle and may constitute a source of structural defects which may affect the performance of the devices during service. For this reason, the formation and evolution of IPs in solder alloys is an issue of fundamental interest.[1] It has been pointed out[2] that systematic investigations are still lacking related to the formation of IPs and especially to the effect of alloying elements on their properties in systems such as Cu-Sn, Ni-Sn, Au-Sn, Ag-Sn, and In-Sn, the binary system with the lowest eutectic point at only 120 °C.

Therefore, we discuss in the present paper alloys from the Cu-Sn-In ternary system, which has gained attention as a potential solder for alternative methods such as transient-liquid-phase-bonding, and for high-performance and/or high-temperature applications. The equilibrium phase diagram of Cu-Sn-In is still under evaluation[3] and only a few systematic experimental studies on the ternary system have been conducted.[4–6] Of particular interest for industry and bonding technologies is the IP called η-phase, which is a stable phase both in Cu-In (Cu_2In) and in Cu-Sn (Cu_6Sn_5) alloys, and is the most common IP found in the interface Cu-solder. The η-phase Cu_6Sn_5 has two structural forms: the high-temperature hexagonal form (NiAs-type) called in the following HT-η and the low-temperature, long-period superstructure with monoclinic symmetry called LT-η, stable below 186 °C.[7] During the soldering process, however, the HT form is usually metastably retained at room temperature, but after subsequent use of devices the HT-$\eta \rightarrow$ LT-η transformation may occur. Such transition is accompanied by a specific volume change of about 2.15%, which is highly harmful for the performance of soldered joints as it produces cracks.[8,9] Defects and impurities may also play a significant role in the stability and kinetics of these phase transformations. To sum up, to make reliable bonds for high-performance technological applications, it turns essential to understand the crystallography, structural properties, stability, and transformation mechanisms of the η-phase and other IPs of the Cu-Sn-In system. The present work focuses on the less-studied ternary η-phase in Cu-rich Cu-Sn-In alloys. We have followed the crystal structure by means of *in situ* thermodiffraction experiments using neutrons, a technique that proved to have major advantages over x-ray diffraction for this kind of metallic systems.[10–13] Phase transitions have also been monitored by differential scanning calorimetry (DSC) measurements. The main objective of the present work is to follow the stability of the η-phase in the temperature range $25\,^{\circ}\mathrm{C} < T < 450\,^{\circ}\mathrm{C}$ for three selected ternary samples.

II. EXPERIMENTAL METHODS

The samples discussed in this work correspond to alloys labeled S4, S5, and S6 in Ref. 13, and their compositions are listed in Table I. The three alloys were annealed at 300 °C

a)gaurelio@cab.cnea.gov.ar.

TABLE I. List of Cu-In-Sn alloys studied in the present work. Nominal compositions and applied thermal treatments are indicated.

	Nominal at. %			
Sample	Cu	In	Sn	Thermal treatment
S4	55	5	40	3 weeks at 300 °C - quenched in iced water Warming to 450 °C at 1.6°/min 30 min dwell at 450 °C
S5	58	12	30	Cooling to 100 °C at 8°/min Warming to 300 °C at 1.6°/min 30 min dwell at 300 °C
S6	60	20	20	Warming to 450 °C at 1.6°/min 30 min dwell at 450 °C Cooling to room temperature

for 3 weeks to promote homogenization, and the ingots were then rapidly quenched to 0 °C. Powders were obtained by manually grinding the ingots for 10 min in an agate mortar.

Neutron thermodiffraction experiments were performed in the D1B two-axes diffractometer at the Institut Laue-Langevin (ILL) in Grenoble, France. The neutron diffractograms were collected placing the ^{3}He multidetector of 400 cells in a cylindrical geometry centered at the sample, with an angular span of 80° and steps of 0.2°. Silicium and alumina standards were used to calibrate the wavelength, yielding the value $\lambda = 2.5275$ Å. Samples measured at high temperature were placed in vanadium-foil sample holders, whereas room temperature measurements were performed using conventional vanadium cylinders of 8 mm diameter. In all cases, the sample holders were almost completely filled with powder. Measurements were performed inside a standard vanadium furnace under a vacuum of 10^{-4} mbar. To accelerate the cooling process, Ar was injected into the furnace between 250 °C and 100 °C before opening the furnace to prevent oxidation.

The neutron flux on the sample was of about 10^6 n/(s cm^2), which allowed us to follow the evolution of the samples on warming by collecting diffraction patterns every 2 min between room temperature and 450 °C with intermediate 30-min dwells at 300 °C. A heating rate of 1.6°/min was applied in all cases. In Table I, we summarize the heat treatments applied to the samples. During the high-temperature dwells, 5-min patterns were added up to enhance the statistics. The diffraction data were qualitatively analyzed and plotted using the LAMP software[14] and then processed with FULLPROF, using models from high resolution neutron diffraction (HRND) data collected at the D2B diffractometer and reported in Ref. 13. Additional bulk material from the same ingots was manually ground to obtain a powder suitable for DSC. Calorimetric curves were collected in Al crucibles using a DSC-2910 TA Instrument under an Ar flow of 120 ml/min. Successive warming and cooling ramps were performed with rates between 2 and 25°/min.

III. RESULTS

A. As-quenched state

The three samples selected for this work had been previously studied using HRND, in their as-quenched state, revealing that at room temperature they are mostly constituted by the HT-η phase.[13] However, we mentioned that the alloys showed certain indications of the presence of some LT-η, too. This second phase was not included in the HRND refinements for several reasons, most importantly because the phase fraction was small and the weak reflections, which distinguish the LT-η from the HT-η were very broad and unresolved, suggesting a small crystallite size. Although such omission was not critical for the systematization of the structural parameters of the primary HT-η phase, it now matters for the analysis of phase transitions and equilibrium conditions in our thermodiffraction experiments, and helps to understand the calorimetric data.

In Fig. 1(a), we recall a magnification of the Rietveld refinement of sample S4 data[13] with nominal 5 at. % In and 40 at. % Sn, measured at room temperature by HRND. The solid line represents a fit using only the HT-η phase with In occupying the *2c* site in the adequate nominal proportion. It is clear that low-intensity data are not completely accounted for using just the HT-η phase (Bragg reflections indicated by vertical bars at the bottom), and neither by the ε-phase, present in some other alloys in Ref. 13. We have highlighted with circles certain regions, to indicate that the single-phase model fails to account for some broad and diffuse reflections. In panel (b), we present a calculated diffractogram for the monoclinic LT-η-phase Cu_6Sn_5 (ICSD card 106530 [Ref. 15]). The diffractogram was modeled using similar experimental conditions, but without modifications in lattice parameters or site occupancies respect to the binary phase. We can see in Fig. 1(b) that the main reflections are common to both the HT-η and the LT-η phases, and that the highlighted regions in (a) are compatible with bunches of weak reflections from LT-η (which in Fig. 1(b) has been modeled only with the instrumental resolution width).

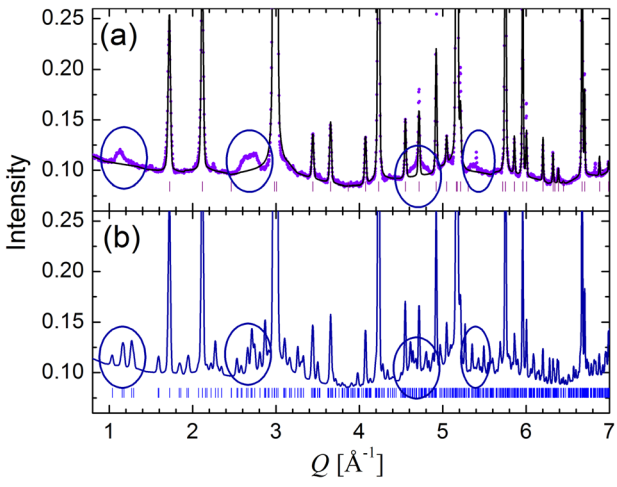

FIG. 1. (a) Rietveld refinement for sample S4 with nominal 55 at. % Cu- 40 at. % Sn- 5 at. % In quenched from 300 °C, from data HRND of D2B diffractometer collected at room temperature using $\lambda = 1.593$ Å.[13] The vertical bars at the bottom indicate the HT-η (hexagonal) Bragg reflections. Major discrepancies between the single-phase model and the D2B data are highlighted with circles. (b) A theoretical diffractogram calculated with the available crystallographic information on LT-η (monoclinic *C2/c*, ICSD 106530) and the same instrumental resolution file from D2B. The circles highlight the same areas as in (a).

B. Phase transformations during heating

Although the S4 sample has already 5 at. % In, it is simpler to analyze its transformations in terms of the binary Cu-Sn phase diagram.[7] In the region of interest, the actual transition temperatures in the ternary diagram may be slightly shifted but the overall picture remains very similar. In fact, the proposed ternary assessment which most closely resembles the current experimental conditions is the 4 at. % In cut between 400 °C and 800 °C compiled by the MSIT, [Ref. 3] which for a 56 at. % Cu proposes the sequence of phases $(\varepsilon+\eta) \rightarrow (L+\varepsilon+\eta) \rightarrow (\varepsilon+L) \rightarrow (L)$ with transition temperatures of 425 °C, 450 °C, and 610 °C, respectively. Such sequence is not unexpected from considerations based on the binaries Cu-Sn and Cu-In equilibrium diagrams, beyond certain discrepancies.

The initial state for our S4 sample is the metastable retention at room temperature of the stable phase at 300 °C. This process is indicated in Fig. 2(a) with an arrow labeled 1. In Fig. 2(d), the thermal history is sketched, highlighting

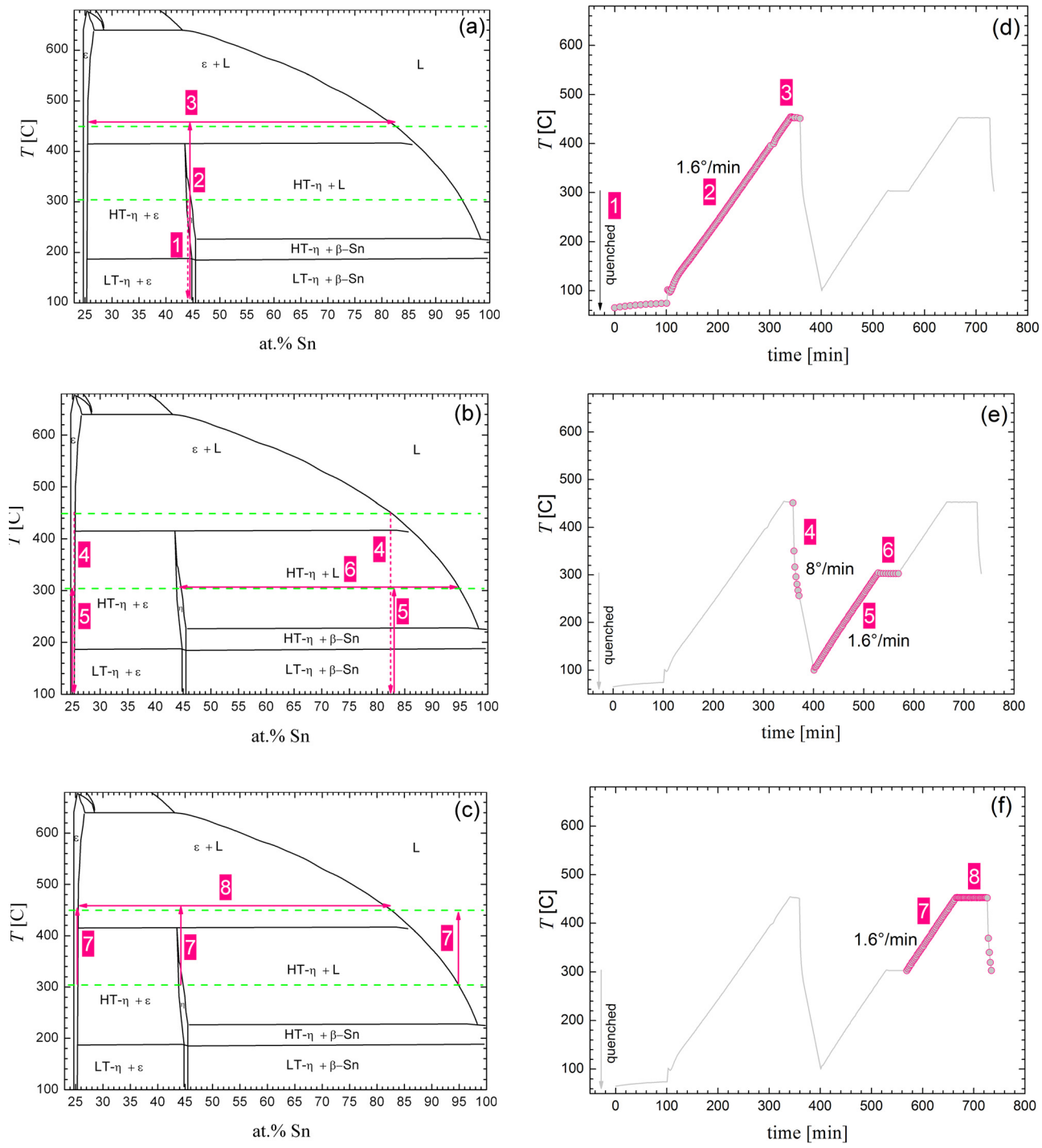

FIG. 2. (a)–(c) Binary Cu-Sn phase diagram after Massalski.[7] The numbered arrows denote the thermal history of the sample during the ND experiments, which correspond to the temperature ramps in the right-hand graphs (d, e, and f). The two temperature dwells at 300 °C and 550 °C are indicated by dashed lines. Dotted arrows indicate quenching or rapid cooling, not allowing for equilibrium conditions to be attained.

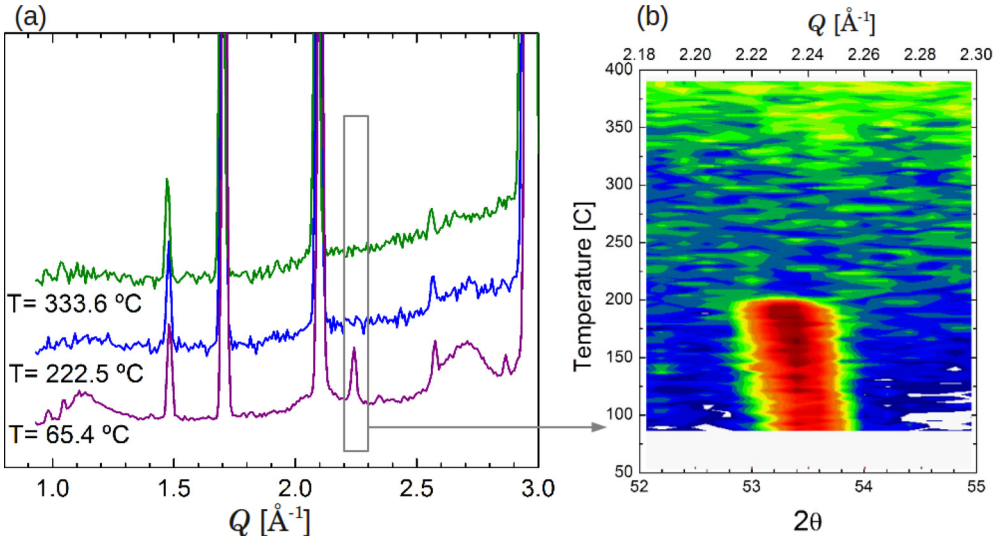

FIG. 3. (a) Magnification of the low-Q region for sample S4 diffractograms collected at different temperatures in instrument D1B using $\lambda = 2.52$ Å. (b) Projection to the $2\theta - T$ plane of the thermodiffractograms showing a Bragg reflection (possibly (1 0 1) from β − Sn), which vanishes between 200 °C and 220 °C. Data were collected on warming with $\lambda = 2.52$ Å between 65 °C and 400 °C.

the relevant stages discussed below. The following stage (2) corresponds to a heating ramp between room temperature and 450 °C. *In situ* diffractograms for this stage show subtle changes around 200 °C. In Fig. 3(a), we present some selected diffractograms in the low-Q region collected at different temperatures for 2 min. We have used a Q scale in Figs. 1 and 3(a) to allow for comparison of diffractograms collected at different wavelengths. At the lowest temperature measured, 65 °C, the D1B data in Fig. 3(a) coincide with the room temperature D2B data (Fig. 1(a)) except for the peaks at 1.48 $Å^{-1}$ and 2.6 $Å^{-1}$, which probably come from the furnace. However, as soon as the sample is heated above 220 °C, a set of peaks vanishes, in particular the wide bumps at 1.1 $Å^{-1}$ and 2.7 $Å^{-1}$, which can be associated to the LT-η as discussed in the previous subsection. Nogita *et al.*[16] also observed using synchrotron XRD the coexistence of the hexagonal HT-η and the monoclinic LT-η phases in Cu_6Sn_5 alloys quenched from 400 °C, the monoclinic phase only being noticed by very weak additional reflections.

DSC measurements of the S4 alloy also evidence small endothermic peaks at low temperature when the as-quenched sample is heated for the first time (black line in Fig. 4). In fact, a closer inspection (inset) reveals that there are two transitions during the first heating ramp. The first peak is around 160 °C, and there is a second one around 216 °C, although both are very weak-indicating the small amount of sample involved in the transformation. Based on the results in Fig. 3(a), we propose that the first peak at 160 °C corresponds to the small amount of LT-η initially present in the as-quenched sample, transforming to the HT-η hexagonal structure. In the literature, the LT→ HT transition is reported at 186 °C for the binary Cu_6Sn_5 [Ref. 4] but had not yet been reported for ternary alloys. The second peak at 216 °C can be associated to the melting point of Sn-rich grain-boundary segregation, as observed in our metallographies presented in Ref. 13. In fact, the temperature evolution of the reflection at $Q = 2.2$ $Å^{-1}$ shown in Fig. 3(b) can be associated to the (1 0 1) Bragg reflection of β−Sn, which has a well-established melting point of 231 °C. This hypothesis will be reinforced by analyzing the subsequent thermal treatments. From the present observations, we conclude that between 150 °C and 220 °C two transitions occur which result in the complete stabilization of the metastably retained HT-η phase.

At higher temperatures, the as-quenched DSC curve (1 in Fig. 4) reveals a further transition which corresponds to HT-$\eta \rightarrow \varepsilon$. In the binary Cu-Sn system, such transition occurs at 415 °C (Ref. 7), and we now show that it shifts to around 467 °C for an In addition of 5 at. % (Fig. 4). The thermodiffractogram for the S4 sample confirms that the transition occurs right at the end of the heating ramp (labeled 2 in Fig. 2). This is illustrated in Fig. 5, corresponding to the final twenty degrees Celsius of ramp 2. Each diffractogram corresponds to an acquisition of 2 min, while the sample was being heated at 1.6°/min. The arrows in Fig. 5 indicate the onset of the crystallographic transition HT-$\eta \rightarrow \varepsilon$. The inset corresponds to a projection on the $2\theta - T$ plane of a selected 2θ range of the diffractograms. We observe that between

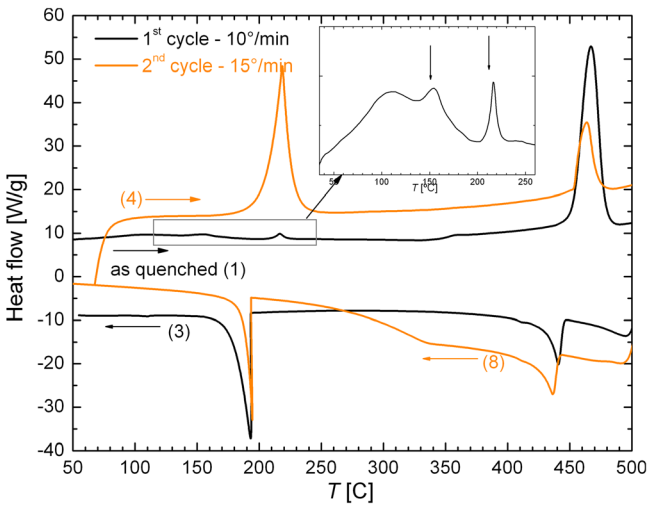

FIG. 4. DSC curves collected on warming for sample S4. The first cycle (dark) corresponds to the as-quenched sample, while the second curve (light) was collected immediately after the fist cycle and corresponds to another thermodynamical state. The curves were obtained under N_2 flow for a heating/ cooling rate of 10°/min (first cycle) and 15°/min (second cycle). Numbers in brackets correspond to the stages represented in Fig. 2.

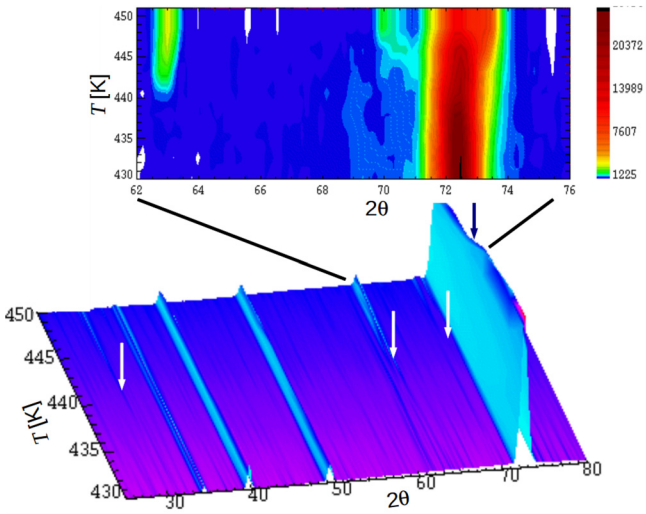

FIG. 5. Thermodiffractogram of sample S4 during the first heating ramp in the range of 430 °C $< T <$ 450 °C. The gradual growth of the ε-phase reflections is indicated with arrows. The inset shows the projection on the $2\theta - T$ plane for a selected region highlighting the onset of ε between 440 and 445 °C.

440 °C and 445 °C, new reflections develop which are consistent with the ε-phase.

According to Ref. 3, an alloy very close in composition to S4, with 4 at. % In and 56 at. % Cu, should already be in a two-phase equilibrium state $\eta + \varepsilon$ at 400 °C, whereas at 425 °C a three-state equilibrium $\eta + \varepsilon + L$ is expected, and finally η should completely transform to an $\varepsilon + L$ mixture at 450 °C. From the thermodiffractograms, we can only obtain information on the solid crystalline phases. What we observe there is that the sample remains in the HT-η phase up to 440 °C, at which the ε phase starts to nucleate, as shown in Fig. 6. The evolution of the diffractograms during the dwell at 450 °C also shows how the system is evolving towards equilibrium, gradually shifting from the HT-η phase to the ε phase. We remark that the reflections marked with arrows in Fig. 6 for the ε phase are indexed within the orthorhombic long-period superstructure of Cu_3Sn (ICSD card 102103), as reported in our previous work.[13] Simultaneously, some melting into a Sn-rich liquid is also expected from the phase diagram, and it can be the cause for the increased background of the diffractograms in Fig. 6.

Stage 4 in the ND experiments (Fig. 2(e)) corresponds to a rapid cooling from 450 °C to room temperature, although due to the furnace inertia, the minimum temperature attained is around 100 °C. The cooling rate does not allow for equilibration, almost as in a quenching process. For that reason, based on the simplified diagram in Fig. 2(b), we expect to find at room temperature a metastable retention of the ε phase plus some quenched Sn-rich liquid (probably in a non-crystalline state). On the contrary, a reversible process would lead to the complete retransformation to the η phase. What we actually observe is the combination of both these situations. On the one hand, a certain amount of η phase is observed along ramp 5, together with the retained ε phase which had not been present in ramp 2, as shown in Fig. 7. On the other hand, the DSC experiment reveals that during the first cooling (analogue to ramp 4, but quicker), the retransformation peak $\varepsilon \rightarrow \eta$ is observed but it is less intense, whereas the Sn-solidification peak at 200 °C has grown considerably. These data support the simplified image of the binary diagram in Fig. 2(b). When heated again (orange curve, labeled 4 in Fig. 4), the melting of Sn is clearly enhanced

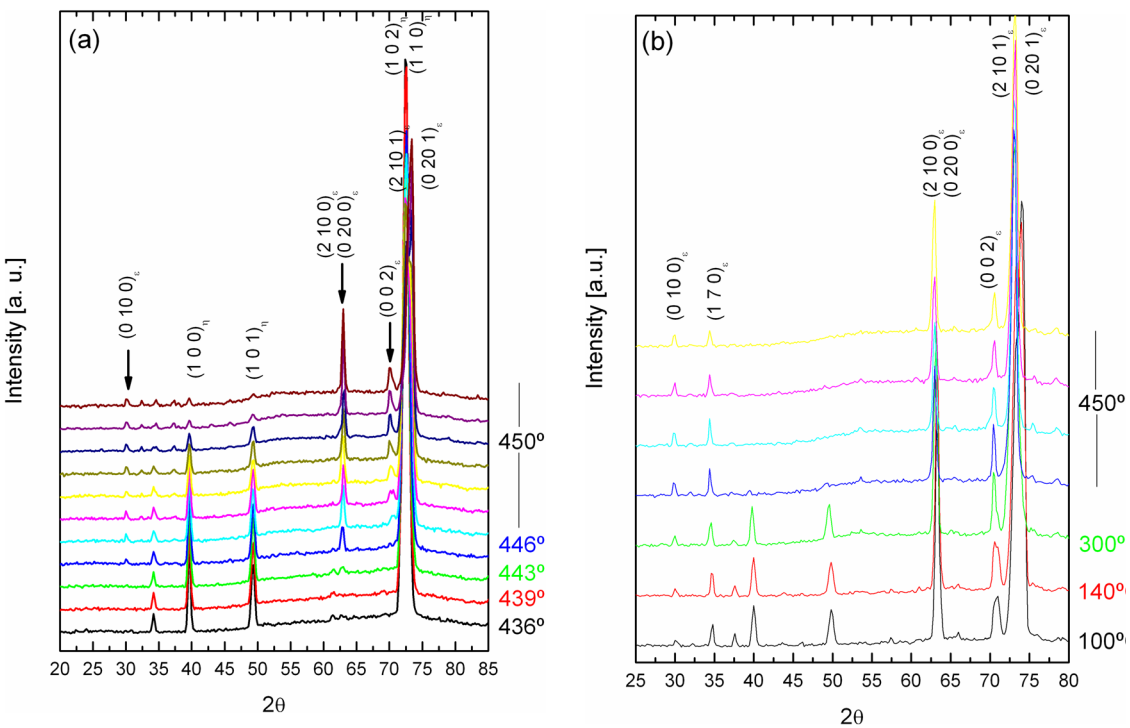

FIG. 6. (a) Sequence of diffractograms collected for S4 at the end of ramp (2) and during the dwell (3) at 450 °C, following the notation used in Fig. 2. The reflections are indexed according to our previous work.[13] (b) Sequence of selected diffractograms between 100 °C and 450 °C (ramp 5–7) and during the last dwell at 450 °C (8).

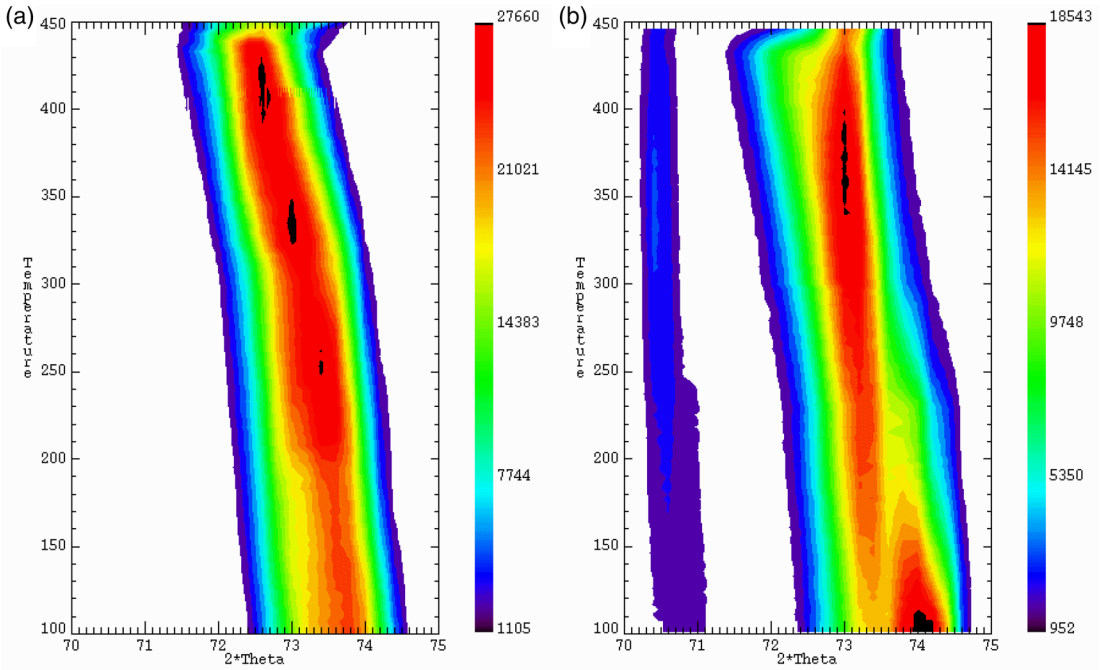

FIG. 7. Comparison between thermodiffractograms obtained for sample S4 during heating ramp 2 (left), and heating ramps 5–7 (right), raising from 100 °C to 450 °C at 1.6°/min, as sketched in Fig. 2. The projection onto the $2\theta - T$ plane is presented for the most intense η and ε reflections.

respect to the first cycle, and this time the melting is also clearly observed in the thermodiffractograms from ramp 5, as an increase in the background. This is illustrated in the projection shown in Fig. 8, in particular in the right-upper corner.

The dwell at 300 °C is labeled as stage 6. According to the diagram in Fig. 2(b), we may now expect a fraction of the sample to remain in the ε phase with a fixed Cu_3Sn composition (left-side of the diagram), and the rest to have a composition around 82 at. % Sn evolving towards $\eta + L$, where L is again a Sn-rich liquid. The thermodiffractograms are compatible with this picture, showing the coexistence of ε and η-phase reflections (Fig. 7(b)). However, the relative intensity of the reflection at $2\theta = 63$ [Fig. 6(b)] results too high with respect to the Cu_3Sn crystallographic model. One possible explanation for this may be in the loss of randomness in the orientation of crystals in the neutron beam. The as-quenched sample had been ground in a mortar to obtain a powder, but the subsequent transformations inside the sample holder can very well lead to a non-uniform distribution of crystal orientations, resulting in intensity mismatches with respect to a perfect powder.

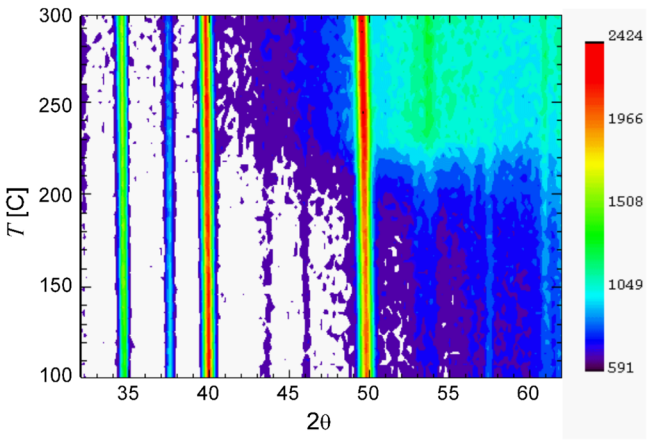

FIG. 8. Projection onto the $2\theta - T$ plane of the thermodiffractograms collected during ramp 5 for the S4 sample. The increase in the background intensity is ascribed to the melting into a Sn-rich liquid at 200 °C.

Further heating to 450 °C (ramp 7) shows the transition from the HT-η phase to the ε phase, and the stabilization of ε during the final dwell at 450 °C (labeled 8) as highlighted in Fig. 6(b). Once more, the DSC curves support this qualitative image, showing during the second and subsequent cycles (not shown) a much greater amount of Sn-rich melting and solidification around 200 °C (orange curve, labeled 2 in Fig. 4) and a less intense peak for the $\eta \leftrightarrow \varepsilon$ phase transformation at 460 °C.

When turning to samples S5 and S6, with 12 at. % In and 20 at. % In, respectively, we arrive at a much simpler scenario, given that the thermal treatment applied *in situ* at ILL was not enough to observe the $\eta \rightarrow \varepsilon$ transformation. For both samples, during ramp 2 there are no changes. The dwell 3 at 450 °C indicates no further modifications, and neither do the following ramps 5 and 7. This is a case of a reversible process with no changes in the constitution and composition of the η phase. DSC curves collected between 20 °C and 500 °C show neither the low-temperature peaks associated to LT-$\eta \rightarrow$ HT-η, melting of tin, nor the high-temperature $\eta \rightarrow \varepsilon$ transition.

IV. CONCLUSIONS

The experimental study of the phase diagram and associated phase transitions in the ternary Cu-In-Sn has become of fundamental technological relevance, given the scarce information available in the literature. *In situ* neutron thermodiffraction

has been used for the first time in this system. The present work offers clear evidence that precise and valuable information can be obtained when this technique is applied carefully, in combination with high-resolution diffraction to correctly identify the phases involved, and with calorimetric experiments to correlate transformation temperatures. Even the most subtle features observed in the thermodiffractograms could be successfully interpreted in terms of the possible phase equilibria proposed in the assessment by Velikanova *et al.*[3] We have shown that the metastable as-quenched state consists mostly of the HT-η phase (but also of some small amount of $\beta - \mathrm{Sn}$) following the sequence of transformations $\eta \rightarrow (\eta + L) \rightarrow (\varepsilon + L)$ with transformation temperatures of 210 °C and 445 °C, respectively. The second heating cycle allowed to further explore the phase diagram after a decomposition at 450 °C. Our results also confirm that a 5 at. % In solubility is possible in the structure of the HT-η phase, with no In segregation as no unexplained reflections were found. Samples with 12 and 20 at. % In were found to remain in a stable single-phase η structure up to 500 °C. Perhaps the most important outcome of the present work is showing that the neutron thermodiffraction technique is a powerful tool to explore this system, allowing precise *in situ* measurements. We believe that this will become a valuable tool in the current process of evaluation of Pb-free solders' phase diagrams.[1]

ACKNOWLEDGMENTS

This work is part of a research project supported by Agencia Nacional de Promoción Científica y Tecnológica, under Grant PICT2006-1947. We particularly acknowledge ILL and the Spanish CRG staff at D1B for the beamtime allocation and technical assistance.

[1]A. T. Dinsdale, A. Kroupa, J. Vízdal, J. Vrestal, A. Watson, and A. Zemanova, "COST action 531-atlas of phase diagrams for lead-free solders," **1**, 182 (2008), available at http://www.univie.ac.at/cost531/.
[2]T. Laurila, V. Vuorinen, and J. Kivilahti, Mater. Sci. Eng. R. **49**, 1 (2005).
[3]T. Velikanova, M. Turchanin, and O. Fabrichnaya, "Cu-In-Sn (Copper-Indium-Tin)," in *Non-Ferrous Metal Ternary Systems*, Selected Soldering and Brazing Systems: Phase Diagrams, Crystallographic and Thermodynamic Data—New Series IV/11C3 (Materials Science International Team MSIT, 70507 Stuttgart, Germany, 2007), p. 249.
[4]W. Koester, T. Goedecke, and D. Heine, Z. Metallkd. **63**, 802 (1972).
[5]S. K. Lin, C. F. Yang, S. H. Wu, and S. W. Chen, J. Electron. Mater. **37**, 498 (2008).
[6]S. K. Lin, T. Y. Chung, S. W. Chen, and C. Horng Chang, J. Mater. Res. **24**, 2628 (2009).
[7]T. B. Massalski, *Binary Alloy Phase Diagrams*, 2nd ed. (ASM International, Materials Park, Ohio, 1990).
[8]K. Nogita, Intermetallics **18**, 145 (2010).
[9]U. Schwingenschlögl, C. D. Paola, K. Nogita, and C. M. Gourlay, Appl. Phys. Lett. **96**, 061908 (2010).
[10]G. Aurelio, A. F. Guillermet, G. J. Cuello, and J. Campo, Metall. Mater. Trans. A **34**, 2771 (2003).
[11]G. Aurelio, A. Fernández Guillermet, G. J. Cuello, and J. Campo, J. Nucl. Mater. **341**, 1 (2005).
[12]J. Martínez, G. Aurelio, G. J. Cuello, S. M. Cotes, and J. Desimoni, Mater. Sci. Eng., A **437**, 323 (2006).
[13]G. Aurelio, S. A. Sommadossi, and G. J. Cuello, "Crystal structure of Cu-Sn-In alloys around the η-phase field studied by neutron diffraction," J. Electron. Mater. (in press).
[14]LAMP, the Large Array Manipulation Program, available at http://www.ill.fr/data_treat/lamp/lamp.
[15]A. K. Larsson, L. Stenberg, and S. Lidin, Acta Crystallogr. B **50**, 636 (1994).
[16]K. Nogita, C. Gourlay, and T. Nishimura, J. Miner. Metals Mater. Soc. (JOM) **61**, 45 (2009).